



# Pixel level spatial variability modeling using SHAP reveals the relative importance of factors influencing LST

Yuhong Hu · Chaofan Wu · Michael E. Meadows ·  
Meili Feng

Received: 11 November 2022 / Accepted: 20 January 2023 / Published online: 16 February 2023  
© The Author(s), under exclusive licence to Springer Nature Switzerland AG 2023

**Abstract** As an important indicator of the regional thermal environment, land surface temperature (LST) is closely related to community health and regional sustainability in general, and is influenced by multiple factors. Previous studies have paid scant attention to spatial heterogeneity in the relative contribution of factors underlying LST. In this study of Zhejiang Province, we investigated the key factors affecting

daytime and nighttime annual mean LST and the spatial distribution of their respective contributions. The eXtreme Gradient Boosting tree (XGBoost) and Shapley Additive exPlanations algorithm (SHAP) approach were used in combination with three sampling strategies (Province—Urban Agglomeration -Gradients within Urban Agglomeration) to detect spatial variation. The results reveal heterogenous LST spatial distribution with lower LST in the southwestern mountainous region and higher temperatures in the urban center. Spatially explicit SHAP maps indicate that latitude and longitude (geographical locations) are the most important factors at the provincial level. In urban agglomerations, factors associated with elevation and nightlight are shown to positively impact daytime LST in lower altitude regions. In the urban centers, EVI and MNDWI are the most notable influencing factors on LST at night. Under different sampling strategies, EVI, MNDWI, NL, and NDBI affect LST more prominently at smaller spatial scales as compared to AOD, latitude and TOP. The SHAP method proposed in this paper offers a useful means for management authorities in addressing LST in a warming climate.

---

**Supplementary Information** The online version contains supplementary material available at <https://doi.org/10.1007/s10661-023-10950-2>.

Y. Hu · C. Wu (✉) · M. E. Meadows  
College of Geography and Environmental Sciences,  
Zhejiang Normal University, Jinhua 321004, China  
e-mail: cfwdh@zjnu.edu.cn

Y. Hu  
e-mail: huyuhong@zjnu.edu.cn

M. E. Meadows  
Department of Environmental and Geographical Science,  
University of Cape Town, Cape Town 7700, South Africa  
School of Geography and Ocean Sciences, Nanjing University,  
Nanjing 210023, China  
e-mail: michael.meadows@uct.ac.za

M. Feng  
School of Geographical Sciences, University  
of Nottingham Ningbo China, Ningbo 315100, China  
e-mail: meili.feng@nottingham.edu.cn

**Keywords** Land surface temperature · Influencing factors · SHAP · Spatial heterogeneity · Zhejiang province

## Introduction

As of 2018, more than 50% of the world's population are located in cities, and this is expected to reach 70% by 2050 (Kulcsár, 2013; Nations, 2018), while in 2020, the urbanization rate in China exceeded 63.89% (Cheng & Duan, 2021). The associated urban heat island (UHI) (Oke, 1982; Peng et al., 2020) has caused a series of environmental problems and health hazards because increased land surface temperature (LST), accentuated by increased frequency of impervious surface areas against the background of global warming (Yu et al., 2019). As cities expand, the interaction between UHIs may induce the superposition effect (Gu et al., 2015), which greatly impacts the thermal environment in a region, augmenting the UHI into a regional phenomenon (RHI) (Chen et al., 2021; Yu et al., 2019). Therefore, UHI mitigation from an accumulated and macroscopic perspective should be considered.

Researchers typically approach the UHI concept as a surface feature (SUHI) or canopy feature (CUHI) (Arnfield, 2003; Hu et al., 2019). CUHI is quantified based on high accuracy weather station data (Li et al., 2017; Venter et al., 2021), but the degree to which these are questionable is influenced by the heterogeneity of urban surface properties and relative quality of the data source (Hu & Brunsell, 2013). In contrast, land surface temperature (LST) derived from remote sensing overcomes many of the limitations of in situ measurements in providing accessibility, broader coverage, and repeat observations (Huang & Wang, 2019; Siddiqui et al., 2021; Wang et al., 2022).

LST has been widely used to investigate the regional thermal environment and is influenced by multiple factors that include climate conditions (Siddiqui et al., 2021; Wang et al., 2022; Xiang et al., 2022), socio-economic indicators (Cui et al., 2016; Zhou et al., 2014), landscape metrics (Hou & Estoqué, 2020; Li et al., 2011; Soydan, 2020; Yu et al., 2020), and biophysical parameters (Li et al., 2020b; Wang et al., 2022; Wolf et al., 2011; Zheng et al., 2016). Previous studies investigating the relationship between LST and its influencing factors typically evaluate the effects of individual features along with traditional correlation-based analyses (Carlson et al., 1994; Gillies & Carlson, 1995; Gillies et al., 1997). Recently, considering the complexity of LST and its nonlinear relationship with potential influencing factors, multi-factor analysis has

been employed (Ezimand et al., 2021; Rongping et al., 2017; Xiali et al., 2018).

Sophisticated algorithms have been developed to reveal the underlying mechanisms that affect spatiotemporal LST change, such as multivariate statistics (Taripanah & Ranjbar, 2021), machine learning (Pouyan et al., 2022), geographically weighted regression (Zhiyu et al., 2019), and convergent cross mapping (Yu et al., 2022) approaches. Machine learning methods may overcome the prior probability distribution requirements of an input dataset using a robust self-regulated learning ability, and are suitable for analyzing nonlinear and complex relations which evaluate nature and strength of the relationship between LST and its underlying factors (Wang et al., 2022). However, their black-box properties are subject to criticism (Li et al., 2021), and there are high level uncertainties in the modeling process, and the included variables may lack interpretation. Given this situation, advanced explanation methods are required to further reveal the spatial variability in regional LST and its underlying factors.

To improve the reliability of modeling, especially in to predictors involved in machine learning methods, the Shapley Additive exPlanations algorithm (SHAP) proposed by Lundberg and Lee (2017) has gained considerable attention (Xin et al., 2021; Yang et al., 2021; Yundong & Hao, 2021). Yang et al. (2021) argue that the SHAP algorithm is beneficial to reveal the factors influencing atmospheric visibility in the Beijing–Tianjin–Hebei Region with improved precision. Stirnberg et al. (2021) used SHAP to realize the separation, quantification, and comparison of meteorological factor impacts on high-pollution episodes. Zhou et al. (2022) and Yu et al. (2020) noted the conditional relationship between LST and landscape metrics using the SHAP method. Nevertheless, previous research has given less attention to the spatial heterogeneity of individual factors provided by the SHAP algorithm, with the exception, perhaps, of investigations of PM<sub>2.5</sub> (Li et al., 2021). Further studies of the spatial heterogeneity of individual contributions to LST using the SHAP algorithm are therefore warranted.

The sampling/scale effect of the function of different factors on LST has attracted considerable attention. Data (feature) selection has been proposed at the local and valley wide level for thermal analysis (Gluch

et al., 2006). A hierarchical approach considering three scales that incorporate the ecoregion, urban cluster, and urban core has been shown to provide the varied cross-scale effects of urban impervious surface on LST (Ma et al., 2016). Zhou et al. (2022) and Tayyebi et al. (2018) also found that the relationship between urban landscape structure and LST varies across different levels of the urban thermal environment. The importance of impervious surface and urban green space changes with scale, from the local urban center to the entire region. However, there is as yet no study that consistently ranks the relative importance of factors such as surface property, background climate conditions, and urban metrics at various spatial scales (Lai et al., 2021), and further research is clearly needed. Considering the continuity and spatial heterogeneity of LST, a sampling scheme that incorporates the whole province, urban agglomeration, and grading of structures within urban agglomerations may be used to explore the corresponding essential factors.

In this study, we combined the SHAP algorithm with the machine learning method to systematically investigate the factors influencing LST in Zhejiang Province, China, with the following main objectives: (1) to characterize the LST distribution within the province, especially in relation to the regions of urban agglomeration and urban centers; (2) to determine the key factors affecting LST at different sampling scales (province — urban

agglomeration — gradients within urban agglomeration); (3) to reveal spatiotemporal heterogeneity of the relative contributions of key influencing factors on LST.

## Materials and methods

### Study region

Zhejiang Province ( $27^{\circ}12'N$ – $31^{\circ}31'N$ ,  $118^{\circ}01'E$ – $123^{\circ}10'E$ ) lies mainly to the south of the Yangtze River Delta in southeastern China and is characterized by a remarkable urban agglomeration (Li et al., 2021). Overall, the province has a subtropical monsoon climate with an annual mean precipitation between 1000 and 2000 mm and air temperature between  $15\text{--}18$  °C (Hanhua et al., 2016). Elevation generally declines from southwest to northeast, with c. 70% of the land is mountainous (“Local Records Office of Zhejiang Provincial People’s Government”) (Fig. 1a). In 2014, the population in Zhejiang Province reached 48,591,800 of which 64.9% was urbanized (Zhejiang Statistical Yearbook, 2015) distributed across three major urban agglomerations (Yiman et al., 2016), viz. the Annulus Hangzhou Bay Urban Agglomeration (AHB), Wenzhou-Taizhou Coastal Urban Agglomeration (WTC), and Central Zhejiang Urban Agglomeration (CZ) (Fig. 1b).

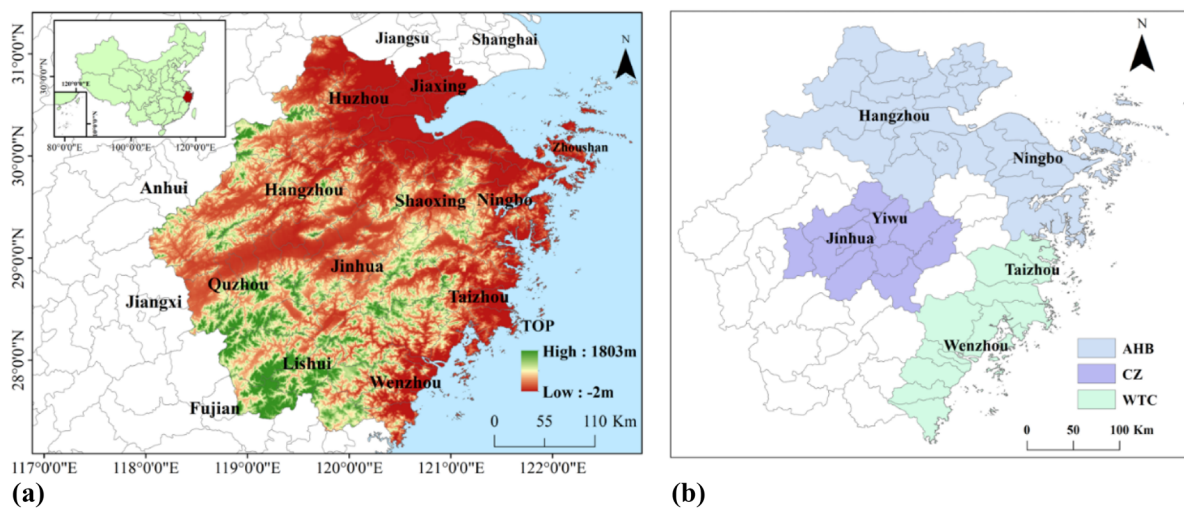


**Fig. 1** **a** Topographic map of Zhejiang Province in China. **b** Composition and spatial distribution of three urban agglomerations in the province

## Data sources

Datasets of the variables, including LST and its influencing factors, were downloaded and collated within the Google Earth Engine platform (<https://earthengine.google.com/>). The variables were classified into three categories: natural factors, socioeconomic factors, and landscape pattern factors (Table 1). The specific technical workflow is illustrated in Fig. 2.

1. LST data in 2014 were derived from the MODIS/Aqua land surface temperature/emissivity 8-day L3 Global 1 km SIN Grid V006 (MYD11A2), monitored at 10:30 h (daytime) and 22:30 h (nighttime) local solar time, at a spatial resolution of 1 km to calculate the annual average temperature.
2. Natural factors. Latitude and longitude were used to represent geographical location. Mean annual rainfall reflects the meteorological environment. Topography obtained from a DEM, with its derivatives: elevation (TOP), slope angle, and aspect, were employed to represent the influence of topography on solar radiation at the land surface (Wolf et al., 2011). Land cover, including

Enhanced Vegetation Index (EVI), reflects vegetation cover (Zheng et al., 2016) and Modified Normalized Difference Water Index (MNDWI) indicates surface water. Albedo, reflecting solar radiation and surface heat storage (Peng et al., 2012), as well as AOD (aerosol optical depth) related to the concentration of atmospheric aerosols were also computed.

3. Socioeconomic factors. Nighttime light data (NL) are frequently used as a proxy for anthropogenic heat emissions (Zhou et al., 2014) and extracted from the data at the Chinese Academy of Sciences' Space and Space Information Innovation Research Institute (<https://www.kepuchina.cn>). POI data (point of interest) containing relevant spatial socioeconomic information were processed by employing the density analysis tool in ArcGIS 10.2. Normalized difference built-up index (NDBI) indicating the distribution of buildings was calculated from the MODIS surface reflectance product (MYD09A1) with a 500-m spatial resolution (the same as MNDWI).
4. Landscape related factors were calculated based on the land cover data, and simplified from 26 classes into five classes, viz., farmland, woodland,

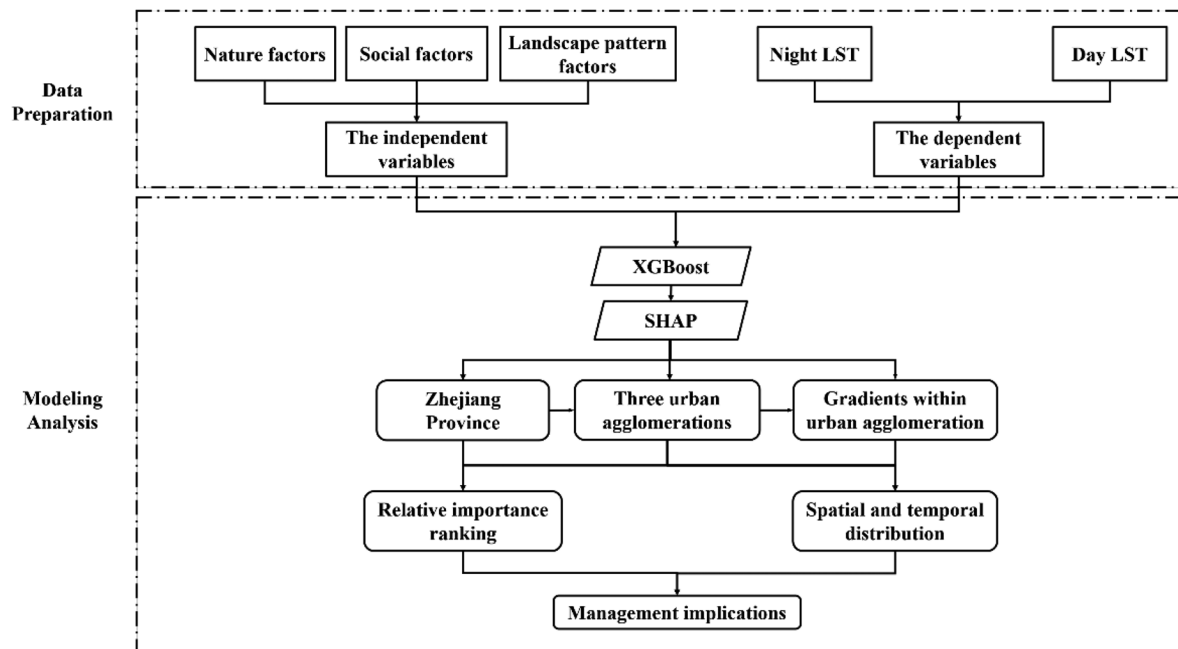


**Fig. 2** Workflow chart

**Table 1** Variables used in this study

Category	Factor	Data source	Temporal/spatial resolution	Reference
LST data	LST	MOD11A2	8-day global 1 km	
Natural factors	TOP	NASA SRTM Digital Elevation	30 m	Li et al. (2020a, b)
	Slope			Shenglong et al. (2017)
	Aspect			
	Enhanced vegetation index (EVI)	MOD13A2	16-day /1 km	Yu et al. (2020)
	Precipitation	National Earth System Science Data Center ( <a href="http://www.geodata.cn/">http://www.geodata.cn/</a> )	1-year/1 km	Hu et al. (2019)
	MNDWI	MOD09A1	8-day/500 m	Maishella et al. (2020)
	AOD	MCD19A2	Daily/1 km	Xiang et al. (2022)
	Albedo	MCD43C3	16-day/0.05°	Xiang et al. (2021)
Socioeconomic factors	NDBI	MOD09A1	8-day/500 m	Maishella et al. (2020)
	Nighttime light	Flint (Chen Fu)	1-year/1 km	Wang et al. (2022)
	GDP (gross domestic product)	Resource and Environment Science and Data Center ( <a href="https://www.resdc.cn/">https://www.resdc.cn/</a> )	1-year/1 km	Xiang et al. (2021)
	POP (population density)		1-year/1 km	Xiang et al. (2021)
	POI	Baidu Map	Kernel density, resample to 1 km	Wang et al. (2022)
	Road density		1 km	
Landscape pattern factors	PLAND COHESION	LUCC	1-year/1 km	Kim et al. (2016)

grassland, water body, and construction land. The proportion and the coherence of each class (cultivated land(P), woodland(F), grassland(G), and construction land(B)) were calculated based on a 10 km × 10 km rectangular buffer zone extracted from the central sampling point (see supplementary files for details of the equations). All data were resampled to the same resolution of 1 km.

## Methods

### *Urban gradient classification*

The sampling framework “Province - Urban Agglomeration -Gradients within Urban Agglomeration” was designed to explore heterogeneity within the contribution of factors across three scales of urban agglomeration. The methodology proposed by Sobrino and Irakulis (2020) was adopted to consider four categories, namely urban center (A), urban adjacent (Su), future urban adjacent (Sf), and peri-urban (Sp),

respectively. Buffer widths ( $W_U$ ,  $W_f$ , and  $W_P$ ) were calculated as follows:

$$W_U = 0.25A^{1/2} \quad (1)$$

$$W_f = 0.25A_{W_U}^{1/2} \quad (2)$$

$$W_P = 1.5A^{1/2} - W_f - W_U \quad (3)$$

where  $A$  represents the area of urban center,  $A_{W_U}$  is the area covering urban center and urban adjacent, and  $W_U$ ,  $W_f$  and  $W_P$  mean the buffer widths of urban adjacent, future urban adjacent and peri-urban, respectively.

### *Extreme Gradient Boosting Tree (XGBoost)*

Machine learning methods have been widely used to model the relationship between predictive variables (influencing factors) and responding variables (in this case, diurnal and nocturnal LST). Compared with

random forest and support vector machine (Yu et al., 2020; Zhou et al., 2022) approaches, eXtreme Gradient Boosting (XGBoost) is an effective ensemble learning method with optimized classifiers based on a gradient lifting framework (Chen et al., 2015), which has improved computing efficiency, higher prediction accuracy and lower computational costs (Fan et al., 2018).

In this study, XGBoost was executed in Python 3.8 using the “XGBoost” package with mean LST as the dependent variable, and the latent features in Table 1 as independent variables. Parameter selection and adjustment were optimized to prevent overfitting and minimize complexity by using the grid search tool. The tenfold cross-validation method was then adopted to evaluate model performance using the coefficient of determination ( $R^2$ ), root mean square error (RMSE), and mean absolute error (MAE).

#### Shapley additive explanation (SHAP)

To interpret the XGBoost modeling process, SHAP algorithm proposed by Lundberg and Lee (2017) was employed to explain the relative global and local importance of participated factors affecting LST using Shapley values computed as follows:

$$\phi_i = \sum_{S \subseteq \{x_1, x_2, \dots, x_p\} \setminus \{x_i\}} \frac{|S|!(p - |S| - 1)!}{p!} [f_{S \cup \{i\}}(x_{S \cup \{i\}}) - f_S(x_S)] \quad (4)$$

where  $\phi_i$  represents the contribution of the  $i$ th feature,  $x$  is the feature values' vector of the instance to be explained and  $p$  is the number of features.  $f_S(x_S)$  represents the prediction of feature values in subset  $S$  that are marginalized over features that are not included in  $S$  (Lundberg et al., 2018).

Next, an additive feature attribution method was used to compute the SHAP value:

$$g(z') = \phi_0 + \sum_{i=1}^M \phi_i z'_i \quad (5)$$

where  $g$  represents the interpretation model,  $z' \in \{0, 1\}^M$ , and  $M$  is the number of total features.  $\phi_i \in R$  indicates the attribution of feature  $i$ .  $\phi_0$  is a constant (Li et al., 2021; Yu et al., 2020). This equation is more simply expressed as:

$$y_i = y_{base} + f(x_{i1}) + f(x_{i2}) + \dots + f(x_{ij}) \quad (6)$$

where  $x_i$  means the  $i$ th sample,  $x_{ij}$  is the  $j$ th feature of  $i$ th sample, and  $f(x_{ij})$  is the SHAP value of  $x_{ij}$ .  $y_i$  represents the predicted target variable, and  $y_{base}$  is the average value of  $y_i$ .

Therefore, local interpretability of the SHAP algorithm arises because of the fact that values vary with location, and this resolves the limitation of traditional methods of evaluating recapitulative importance whereby values are obtained across an entire region and individual pixels are not resolved (Li et al., 2021). In this study, the local interpretation of SHAP was used to explore the pixel level (1 km) spatial contribution heterogeneity of factors influencing LST.

## Results

### Spatial distribution of land surface temperature

Three sampling levels were proposed to feature the spatiotemporal LST distribution, i.e., the whole province (Fig. 1a), three urban agglomerations (Fig. 1b) and four gradients within each of the urban agglomerations (Fig. 3).

Overall mean daytime and nighttime temperatures were 20.33 °C and 11.03 °C. As Fig. 4 reveals, daytime and nighttime LST values were generally lower

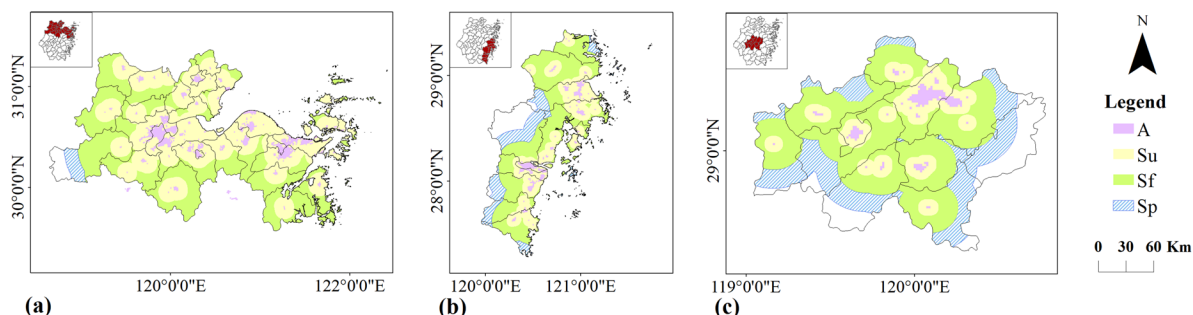


**Fig. 3** Gradients within the three major urban agglomerations: **a** in AHB; **b** in WTC; **c** in CZ

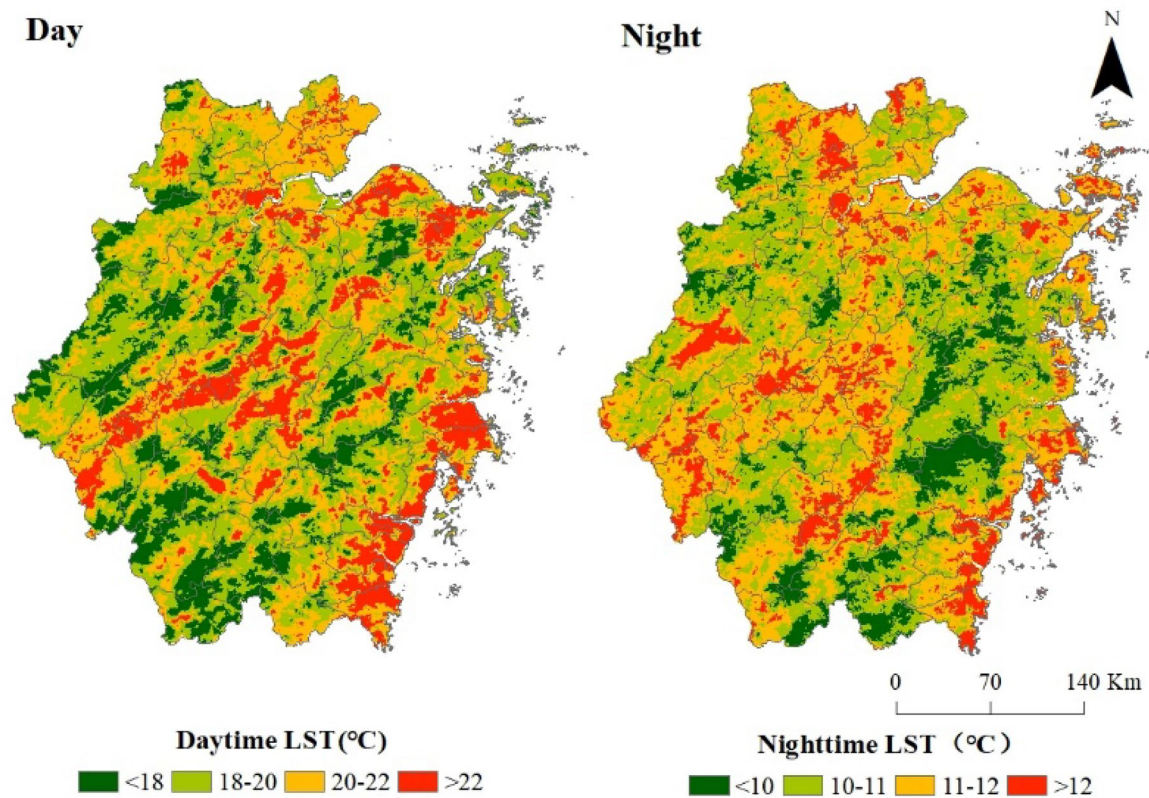


**Fig. 4** Spatial distribution of day and night land surface temperature in Zhejiang province

in the southwest and higher in the northeast of the province. High-temperature spots are observed in the central Jinqu Basin, the eastern coastal areas, and in urban centers including the capital city Hangzhou. Cooler localities are mainly in the mountain areas.

The LST values in Table 2 reveal that all the urban centers have the higher LST when compared to urban agglomeration, especially to the whole province. WTC holds the highest temperature and AHB has the lowest. The standard deviation values indicate that the daytime heterogeneity is observably higher than night.

Comparing LST values within the four gradients among AHB, WTC, and CZ (Fig. 5), it is observed that daytime and nighttime mean temperatures for three urban agglomerations all decreased away from the urban center. AHB exhibits the lowest mean LST in every gradient except Sp at night, while the highest temperatures in the urban center zone are for WTC.

Overall, higher LST values are generally found in the central urban area, both across the whole province and among the three urban agglomerations. LST gradually declines outwards towards the peri-urban

**Table 2** Statistics of day and night LST at different sampling scales (°C)

	Zhejiang Province	Urban agglomerations			Urban centers		
		AHB	WTC	CZ	AHB	WTC	CZ
Day	Mean	20.34	20.29	20.92	20.07	22.68	24.56
	Std dev.	1.77	1.57	1.85	1.87	1.15	1.09
Night	Mean	11.03	11.06	10.74	11.13	11.88	12.25
	Std dev.	0.93	0.89	0.99	0.86	0.67	0.73

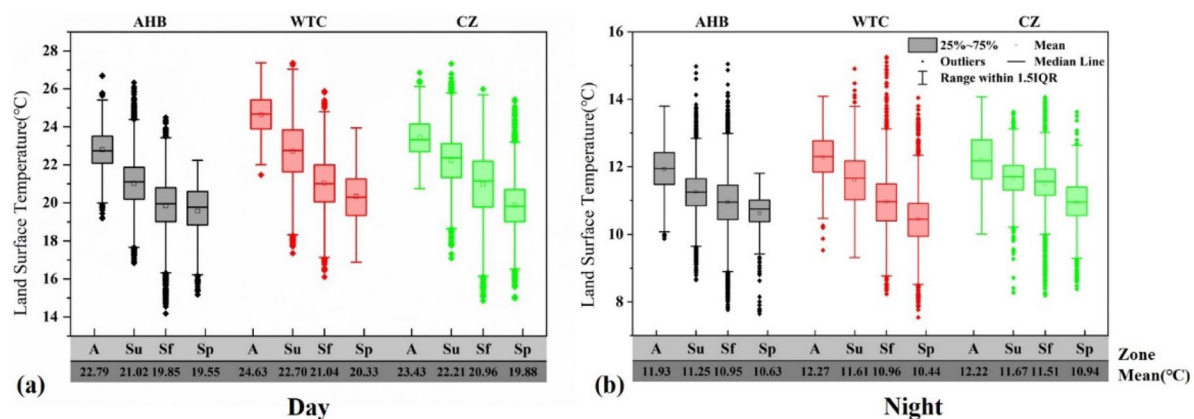


**Fig. 5** Boxplot of day and night LST values within four urban gradients for the three urban agglomerations in Zhejiang Province

areas. However, although AHB has the greatest degree of urbanization (58.8%, compared to WTC, 28.8% and CZ, 21.2%), LST values here are not the highest, and this agglomeration even exhibits lowest daytime values for each gradient.

#### The relative importance of LST factors

In this study, the XGBoost model optimized with the tenfold cross-validation method combined with SHAP algorithm were adopted to explain the key factors affecting LST. The distribution of  $R^2$ , RMSE, and MAE values (Table 3) indicate that the modeling process acquired acceptable results, and that this lays a sound foundation for analyzing the relationship between LST and selected factors based on the SHAP values. Accordingly, the relative importance of influencing factors on different sampling levels can be compared.

Mean absolute daytime and night SHAP values at the provincial scale were ranked (Fig. 6). Among the daytime LST influencing factors, latitude is the most important determinant and has the highest global SHAP value. This is followed by the topography factor (TOP) and socioeconomic factors

(nightlight and NDBI). Latitude is also the most important influence on nighttime LST, although the order of importance thereafter changes to longitude, AOD and EVI. In general, natural factors are most influential during both daytime and nighttime, although factors related to human activity are notable determinants of daytime LST and landscape factors at night. Note that, since SHAP values depend largely on the standard deviation of LST (Eq. 6), the results show that daytime SHAP values are distinctly more variable than those at night, even for the same factor.

From the perspective of urban agglomerations, the absolute mean values of SHAP indicate that the most influential factors of LST are latitude and longitude in the daytime and at night, although the order of the other top 10 factors is different (Fig. 7). In the daytime, the top four factors were the same for all agglomerations, although the effect of slope, POI and EVI in AHB, aspect and Albedo in WTC as well as TOP in CZ, were more prominent when compared to the provincial scale. At nighttime, the rank order differed between agglomerations more markedly. The impact of vegetation related features, including EVI, F\_pland, and F\_cohesion is greater in AHB. The effect of distance to the sea (longitude) and elevation (TOP) on LST appears to be greater in WTC, while for CZ, distance to the sea, vegetation (EVI), and air quality (AOD) are more important factors than at the provincial scale.

Figure 8 shows the relative importance of different day and nighttime LST factors across the four

**Table 3** Results of the tenfold cross-validation evaluation indices

	$R^2$	RMSE (°C)	MAE (°C)
Day	0.93	0.49	0.38
Night	0.90	0.32	0.24

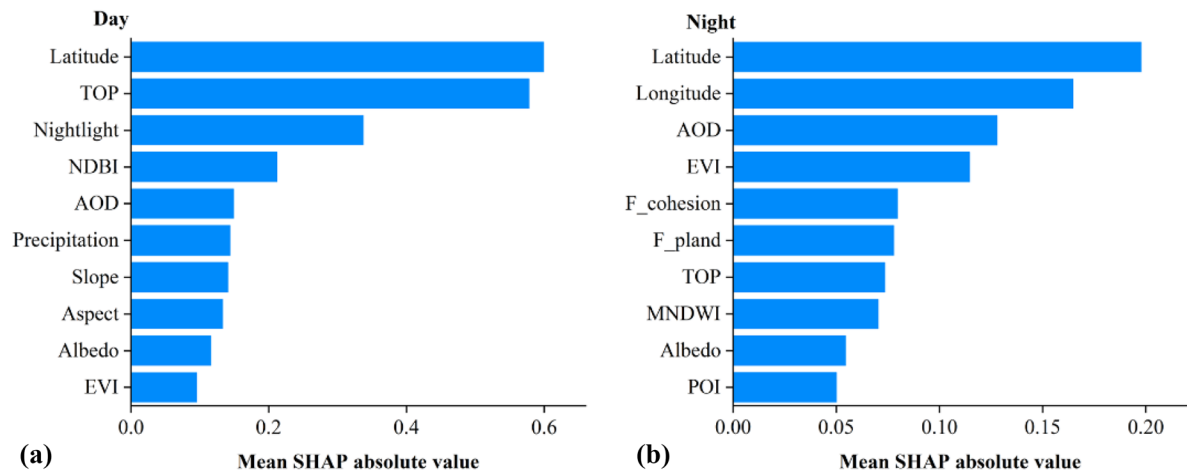


**Fig. 6** The relative importance of the top 10 influencing factors for day and night LST in Zhejiang Province

gradients (A-Su-Sf-Sp) for the three urban agglomerations. In the daytime, the most significant natural factors in the urban center are TOP (AHB, CZ) and latitude (WTC). Socioeconomic factor NL exhibits the highest SHAP values. Its contribution decreases from A to Sp, although the SHAP value for Sp is greater than for Sf, which means that the effect of

human activities on LST decreases from the urban centers outwards, albeit that minimum values are not found in periphery. At night, the impact of anthropogenic factors is weaker and natural and landscape characteristics appear to be more effective. EVI is evidently important in A, as is MNDWI. Latitude remains a clear LST determinant across the gradients,

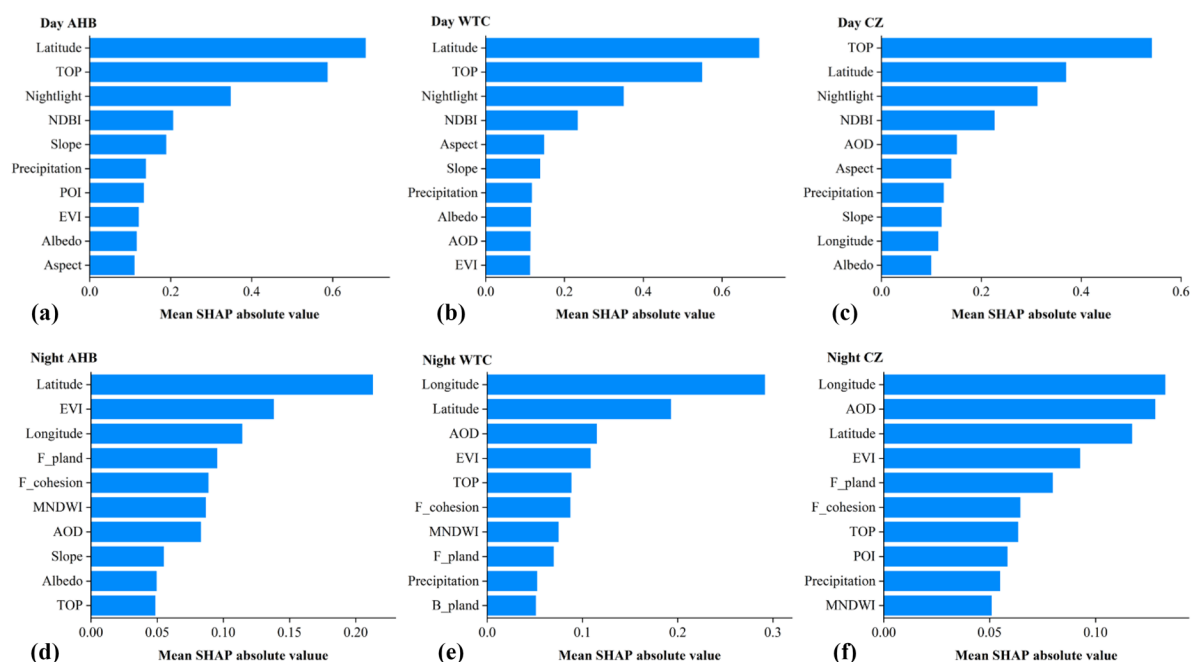


**Fig. 7** Rank order of the mean absolute SHAP values for top 10 factors: **a** daytime in AHB; **b** daytime in WTC; **c** daytime in CZ; **d** nighttime in AHB; **e** nighttime in WTC; **f** nighttime in CZ

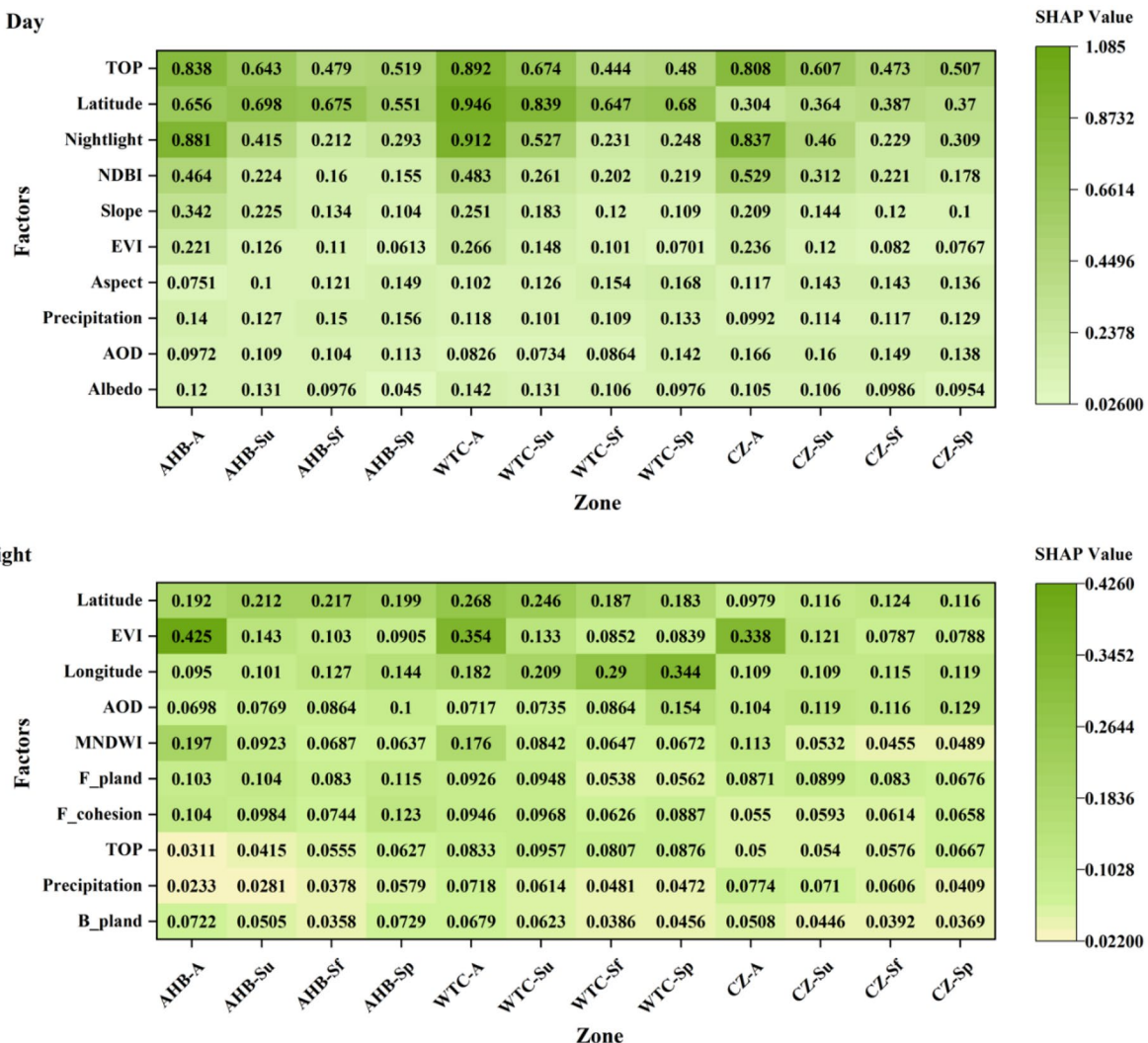


**Fig. 8** The relative importance of the top 10 influencing factors for day and night LST within gradients. Darker green represents greater importance

while AOD evidently exhibits greater impact on Sp compared to A for all three agglomerations. It is noteworthy that F\_pland and F\_cohesion, representing the percentage of forest land and intactness of the forest landscape play a more substantial role on night LST in Sp than A in AHB, as indicated by their higher SHAP values ( $> 0.1$ ).

While the relative importance of LST drivers does vary across the province, natural factors are consistently the most influential, especially latitude. Since AHB lies furthest to the north, LST values are close to the lowest. Nightlight, which is a proxy for the intensity of anthropogenic influence, exhibits the

largest contribution to daytime LST in the urban centers within the three urban agglomerations. At night, with lower levels of human activity, the importance of socio-economic factors declines and landscape and other natural factors, including EVI, MNDWI, and AOD, are more clearly influencing LST.

#### *Spatial distribution of SHAP values for key factors*

According to the SHAP values for all factors, the most significant natural drivers (longitude, latitude, TOP, EVI, AOD), socioeconomic factors (nightlight, NDBI) and landscape metrics (F\_pland, F\_cohesion) were selected

to map the spatial variation of their respective contributions on day and night LST against the background of high levels of urbanization. The overlay of SHAP distribution and gradients (Figs. 9, 10 and 11) within the urban agglomerations across the province indicates that the influence of different LST factors varies spatially.

The relative importance of longitude and latitude exhibits a series of sub-parallel zones (trending N-S in the case of longitude, and E-W in the case of latitude). In the day, longitude exhibits a positive impact on LST in the east-central region, especially for the basin areas (Fig. 9a), while at night, the effect is reversed (Fig. 9f). The influence of latitude on daytime LST (Fig. 9b) exhibits more spatial heterogeneity than that at night (Fig. 9g).

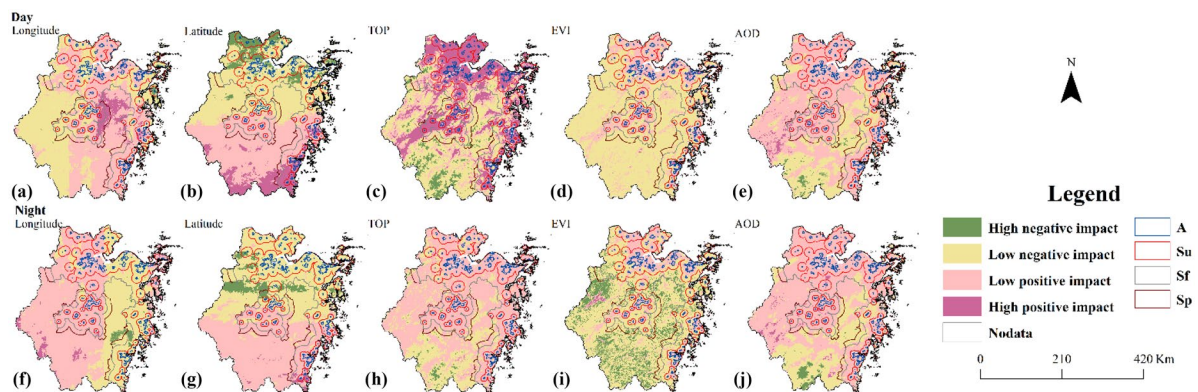
TOP exhibits a positive impact on the daytime LST in the south, occupying almost all AHB as well as A and Su of WTC and CZ (Fig. 9c), although its contribution on LST clearly decreases towards the southwest, where its effect is negative (Fig. 9h). For EVI, positively impacted regions are located in A and Su both in the day and at night, and its negative impacts are especially clear in the mountainous regions (Fig. 9d, i). Regarding AOD, SHAP values are similarly distributed in both day and nighttime, with negative impacts especially in Sp and in other higher altitude localities (Fig. 9e, j).

Figure 10a illustrates that daytime SHAP values for nightlight exhibit positive effects on urban areas, especially in WTC and AHB, while there are negative

values in the mountains to the south (Fig. 10a). In contrast, the spatial pattern of values for NDBI is rather fragmented (Fig. 10b). Positive values are observed within A and Su, especially the urban centers, but the southwest mountain region is more markedly affected by daytime NL than NDBI, although their relative contributions at night were much lower with no highly impacted regions (Fig. 10c, d).

SHAP values for the key landscape metrics, F\_pland and F\_cohesion (Fig. 11) indicated that the importance of the two factors is similar for day and night, albeit that the pattern is more strongly evident in the former. Referring to the bitemporal relative importance values presented in Fig. 6, this has a positive impact at night, although A and Sp are affected negatively (Fig. 11c, d).

Overall, the pixel-based maps of these key factors' SHAP values facilitate the spatial distribution of contributions to LST by various factors. The impacts of longitude and latitude on LST are independent from the development of urban areas, but TOP, NL, NDBI exhibit close relationships, namely, low altitudes along with higher nightlight and NDBI values indicating intensive human activities were positively impacted. In the urban center, F\_pland and F\_cohesion cooled the LST, but EVI warmed in the daytime. At night, they all had positive impacts on LST in A. Comparing the relative importance of wood landscape indices with EVI suggests that the latter makes greater contributions to the LST.



**Fig. 9** Spatial variations of day and night SHAP values for natural factors as follows: **a** longitude in the daytime; **b** latitude in the daytime; **c** TOP in the daytime; **d** EVI in the daytime; **e**

AOD in the daytime; **f** longitude at night; **g** latitude at night; **h** TOP at night; **i** EVI at night; **j** AOD at night

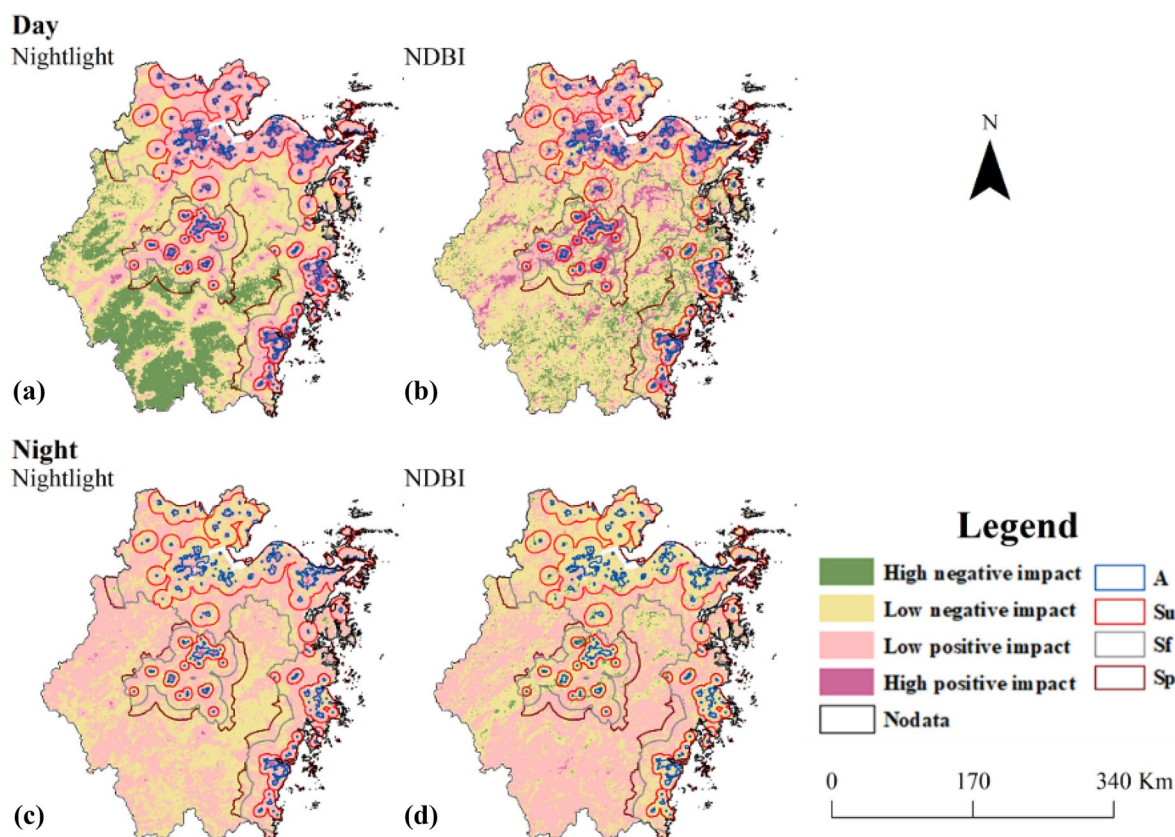


**Fig. 10** Spatial variations in day and night SHAP values for socioeconomic factors as follows: **a** nightlight in the daytime; **b** NDBI in the daytime; **c** nightlight at night; **d** NDBI at night

## Discussion

Along with previous studies that have demonstrated local LST to be closely related to the degree of urbanization (Tayyebi et al., 2018; Wang et al., 2022, 2021a, b; Yang et al., 2021, 2022), this study indicates that urban centers are associated with higher temperatures, especially when compared with higher elevation regions in Zhejiang province. However, the spatial distribution of LST is heterogeneous and influenced by various factors, and even areas within the same urban agglomeration may show contrasting effects.

### Spatial distribution of the contribution of key factors to LST based on SHAP

The SHAP results reveal a high degree of spatial heterogeneity across the province and cast light on

factors underlying LST that would be missed in conventional spatial analysis.

Among the most important natural factors, the distribution of individual SHAP values indicates that longitude and latitude vary in sub-parallel zones at the provincial scale (Fig. 9a, f). This points to the significance of geographical location rather than the degree of urbanization, especially in the case of latitude.

TOP has a negative relationship with temperature, since the environmental lapse rate determines that temperature decreases with elevation (Chen et al., 2012; Tayyebi et al., 2018; Xiang et al., 2021; Zhi et al., 2020; Zhou et al., 2014). Human settlements are often preferentially located at lower altitudes, for example, along river valleys, and so the result is as expected.

The distribution of SHAP values for AOD indicates positive impacts of aerosol on LST are in

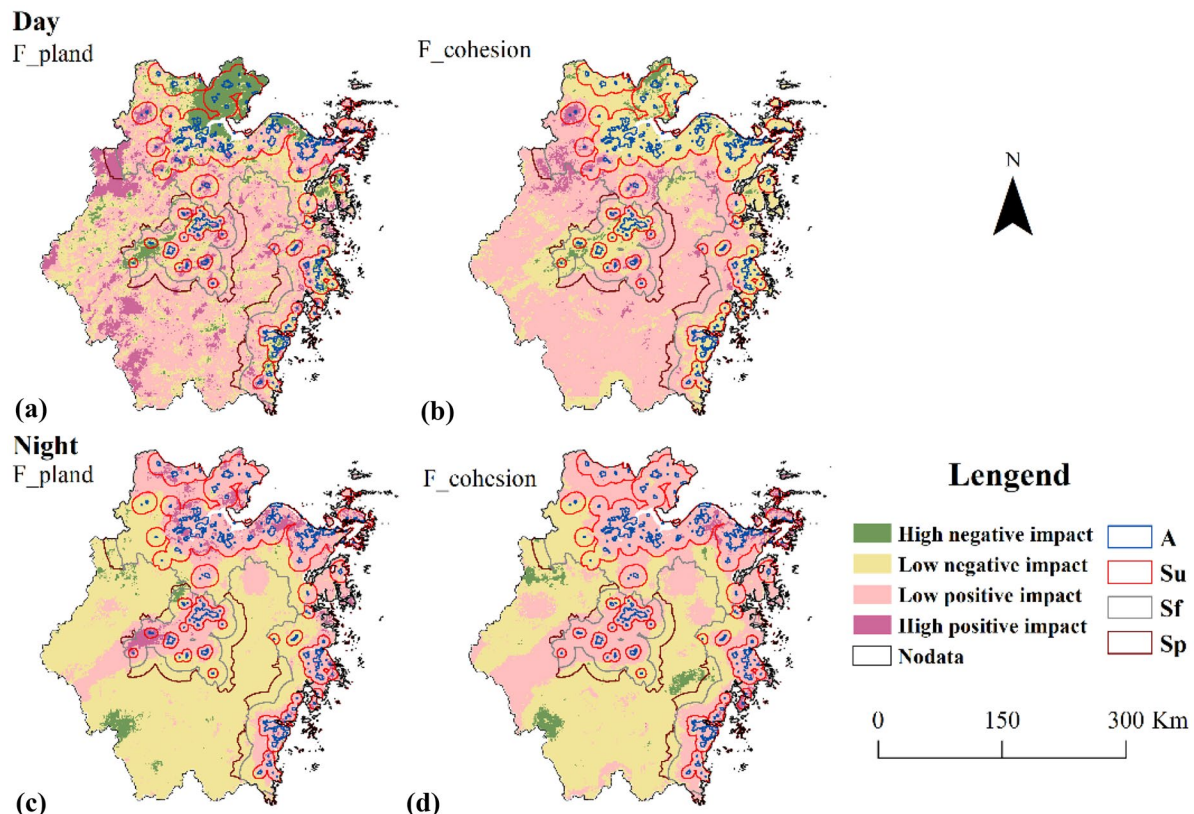


**Fig. 11** Spatial variations of day and night SHAP values for landscape indices as follows: **a** F<sub>pland</sub> in the daytime; **b** F<sub>cohesion</sub> in the daytime; **c** F<sub>pland</sub> at night; **d** F<sub>cohesion</sub> at night

regions of high aerosol concentration, including A, Su, and Sf of CZ and A of AHB, both in the day and at night. AOD values in the industrial region of the Jinqu Basin are observed to be especially high, and our results show a strong warming effect on LST during the day (Fig. 12(III)). On the other hand, AOD appears to have a negative effect in higher altitude localities (Fig. 12(I)). Previous studies had failed to achieve consensus regarding the influence of AOD on LST, with some considering a positive effect (Kim, 2019; Xiang et al., 2022), while others still suggest a negative correlation (Jin et al., 2010; Siddiqui et al., 2021). The impact of aerosols on climate depends not only on the quantity of aerosols but also on their optical properties which both affect LST through reducing solar radiation reaching the surface. However, scattered aerosols have a cooling effect as they reduce the energy received at the surface, whereas there can also be a warming effect, since the suspended particles absorb reflected longwave radiation (Karnieli

et al., 2010; Yu et al., 2022). Consistently, cooler and cloudier conditions over higher ground (Fig. 12(I)) are associated with abundant water vapor aerosols, which easily induce Mie scattering (Li et al., 2022), thereby reducing LST. In contrast, AOD positive effects are exhibited in lower elevation regions where human activity is more intense (Fig. 12(II)) and characterized by anthropogenic emissions of absorptive aerosols (Yu et al., 2022).

EVI is shown to positively affect LST in the inner areas of urban agglomerations (Fig. 9d, i), but the impact varies (Fig. 13). Most previous studies simply present the impact of EVI on LST as negative because of shading and transpiration (Li et al., 2011; Peng et al., 2012; Zhou et al., 2014). However, the nonmonotonic trend reported here implies that the effect of EVI is different according to land use and has a more variable effect on LST (Fig. 13a, b). For example, when vegetation is around water bodies (Fig. 13(I)), the effect on LST is negative in the

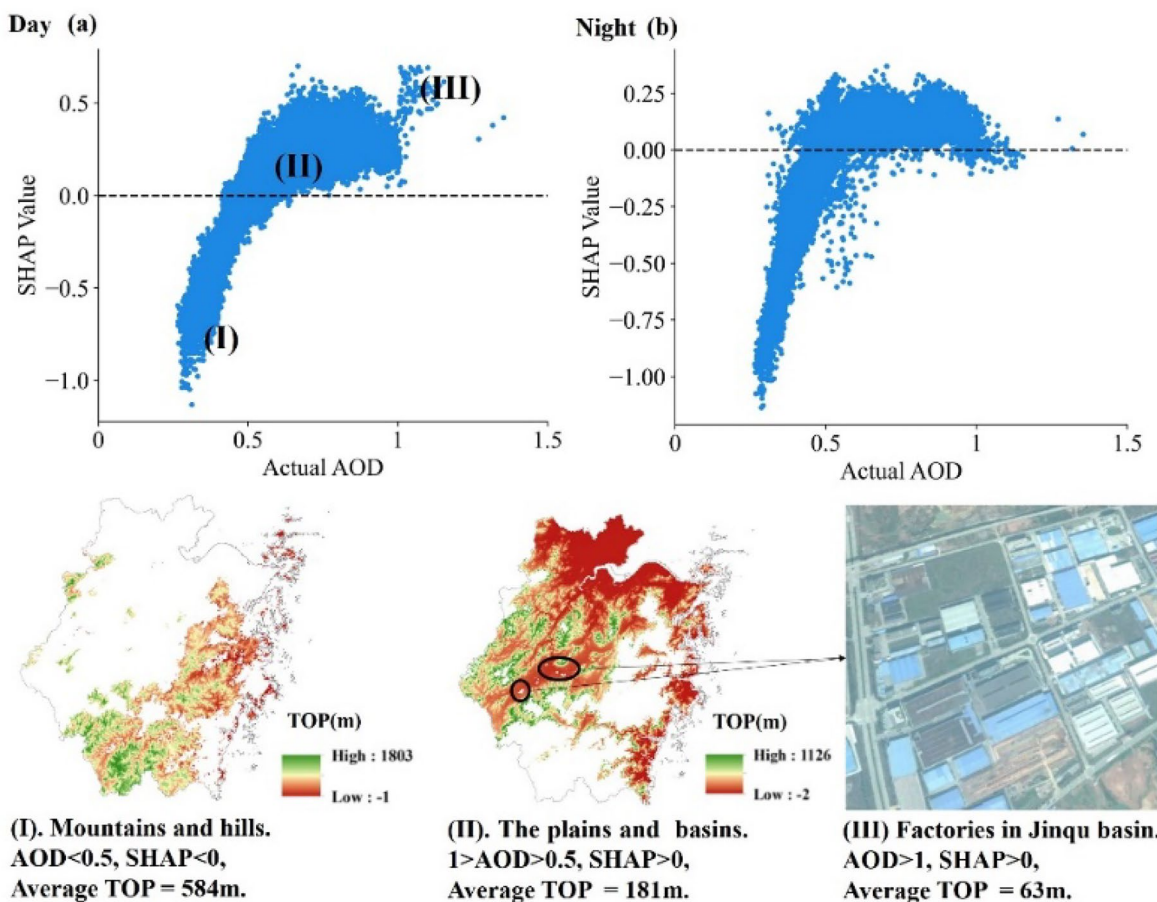


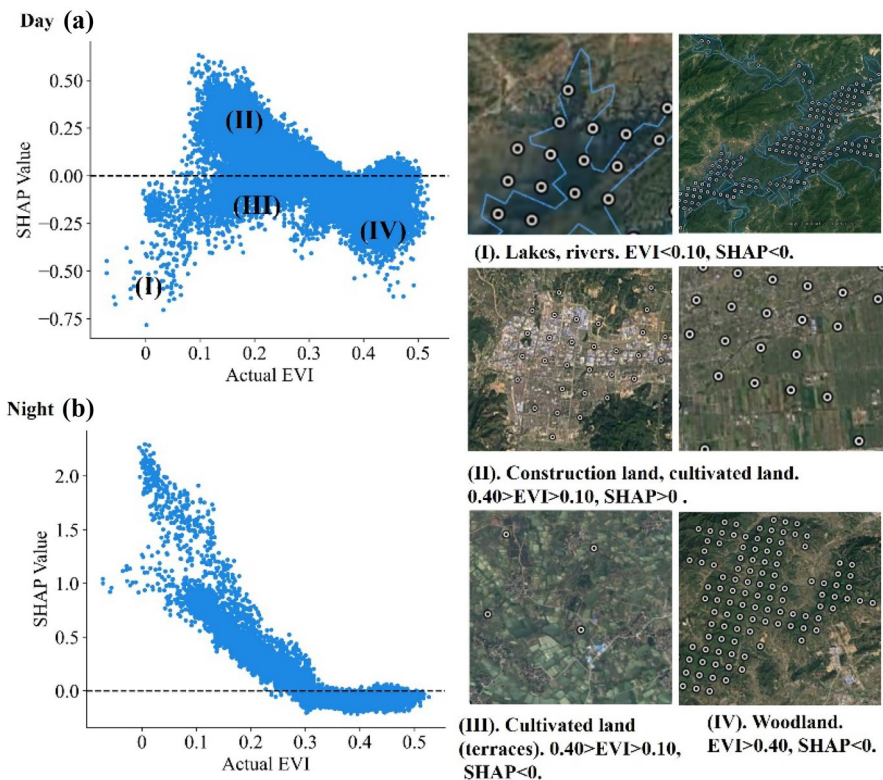
**Fig. 12** SHAP dependency plots for AOD in Zhejiang province with typical samples' TOP and Google Earth images

day but positive at night, a situation similar to what occurs in paddy fields (Fig. 13(III)). EVI always has a warming impact in the urban center which is largely built-up (Fig. 13(II)). As for woodland (Fig. 13(IV)), in the daytime, they have stronger negative effects, but at night, the impacts are not obvious because the values are near zero.

During the daytime, factors related to human activities, i.e., nightlight and NDBI both exhibit a positive effect on LST in the urban center (Fig. 10a, b). This effect is widely reported (Logan et al., 2020). However, consistent with other studies (Liu et al., 2021), the contribution of NL is more important than that of NDBI (Fig. 6a). When NL is low, SHAP values are negative, but they become positive when NL is larger in the daytime (Fig. 14a), and the relationship is

more U-shaped for the nighttime situation (Fig. 14b). In addition, the relationship for NL (Fig. 6) exhibits a better fit with daytime LST, a result consistent with previous findings (Li et al., 2019; Xiang et al., 2021). NL reflects human activities (Li et al., 2020a, b) with higher intensity during the day than that at night, a suggestion supported by nighttime SHAP values which are generally very low, indicative of only marginal effects (Fig. 14b). Furthermore, localities with small NL values and large negative SHAP values (Fig. 14(I)) are associated with lakes and rivers, which have increased nighttime LST on account of their larger specific heat capacity. The positive effects on LST of places where NL values are greatest are especially obvious in built-up major urban centers (Fig. 14(II)).

**Fig. 13** SHAP dependency plots for EVI in Zhejiang province with Google Earth images of typical places according to EVI values



#### The effect of sampling framework on the relative importance of key factors

Fine sampling framework based on the spatial distribution of SHAP values, whereby we identify three different levels (province–urban agglomerations–gradients), was adopted to compare the relative importance of key factors in the province. The rank order of the most prominent factors within urban agglomerations and their inner gradients was computed (Figs. 6, 7, and 8).

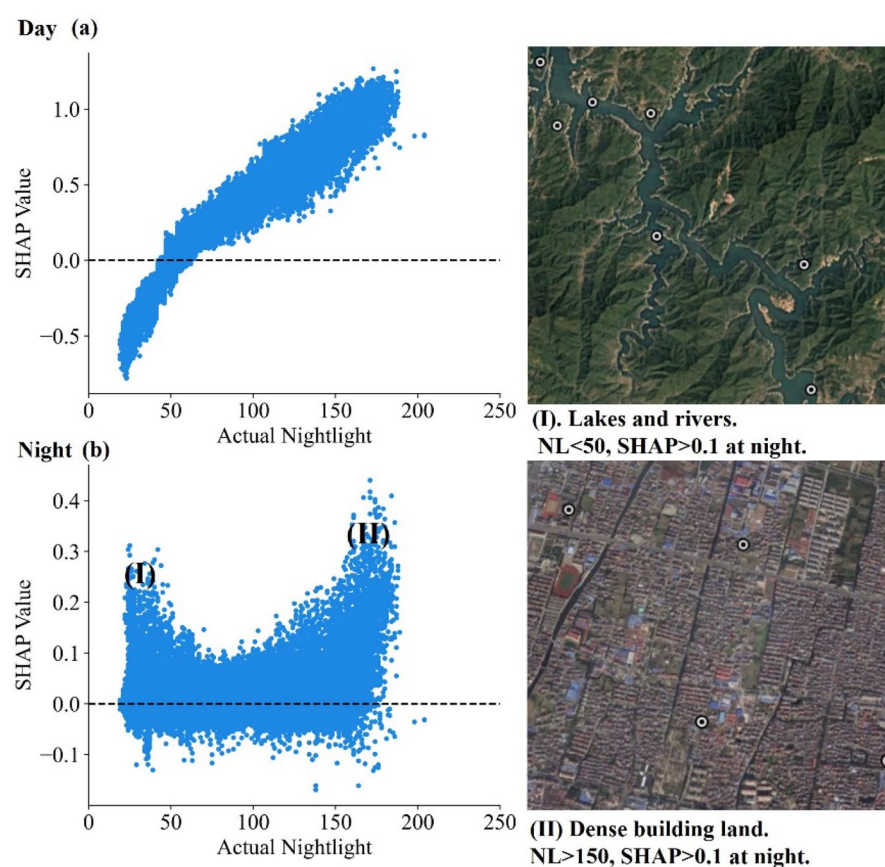
Latitude emerges as the most important LST driver across the province, although its SHAP value is highest within the urban agglomerations. Among all the gradients, latitude is most influential in the urban center of WTC. Therefore, although Wang et al. (2021a) reported that latitude had little impact on LST at the scale of the individual city, here, we note that the spatial scale at which the study is made is important.

Similarly, when comparing the SHAP values of TOP among the different scales, we show that urban centers situated in areas with relatively homogeneous

flat terrain have the most prominent effect on LST, followed by the provincial scale. The contribution of urban agglomerations is stronger in CZ than in AHB and WTC, while the importance decreases in general from the urban center to the suburbs. The scheme of sampling in this study contrasts with previous studies, which have in general focused on whole areas (Yuanhong Deng et al., 2018; Sharma et al., 2018).

AOD is also shown to influence LST dissimilarly. For the whole province, AOD becomes one of the most critical factors affecting nighttime temperature (Fig. 6b). Among the three urban agglomerations, the SHAP value of AOD in CZ is higher than that of the entire province (Fig. 7f), probably due to the location of CZ in the Jinqu Basin where air circulation is restricted, and aerosol concentrations are elevated there. Within the gradients, SHAP values of AOD in Sp in CZ and WTC are the highest. Previous studies pay scant attention on the contribution variation of AOD for different scales (Karnieli et al., 2010; Kim, 2019; Xiang et al., 2022). For instance, Siddiqui et al. (2021) just analyzed the quantity change of AOD

**Fig. 14** SHAP dependency plots for NL in Zhejiang province with Google Earth images of areas typical of NL values



and SUHI in urban and non-urban areas, ignored the impact change of AOD on LST in different regions.

By comparison, variables EVI, MNDWI, NDBI, and NL all exhibit greater influence at smaller scales. The SHAP values of EVI in AHB are distinctive compared to other urban agglomerations and across the province as a whole. The greatest contribution of these factors to nighttime LST is in the urban center, as reported also by Geng et al. (2021) and Liu et al. (2021) who note the strong impact of EVI in more developed cities. The contribution of MNDWI to nighttime LST in the urban center ranked only second to EVI as the cooling subject by convection (Cai et al., 2018). Rivers decrease local temperature at distance of 45.5 m strongly (Yunfang et al., 2018). For Zhejiang province, because of the relatively small proportion of water bodies (about 10%), the importance of MNDWI at the provincial scale is not obvious. However, many cities have rivers running through them, and, therefore, the impact of this factor in the urban centers may be more marked.

NDBI is most influential in urban centers, an observation supported by other studies (Wang et al., 2022). The high proportion of impervious surfaces in cities absorbs incoming solar radiation and releases thermal energy into the surrounding atmosphere (Coutts et al., 2007). Here, we show that built-up land use is not the most important influence at night (Fig. 6), an observation also made by Mathew et al. (2022) who also found the correlation between NDBI and LST to be stronger in the daytime. Indeed, NDBI is even negative in A and Su (Fig. 10d). Bala et al. (2020) noted the negative correlation of NDBI with LST at night and concluded that resulted from the misclassification of bare land as built up, while it has a different thermal response to buildings. Moreover, building materials may significantly influence LST and produce even opposing effects (Liu et al., 2011), while Deng et al. (2021) note that roof color also impacts LST. Interactions between NDBI and nocturnal LST are therefore complex and inconclusive.

NL also exhibits greater impact on daytime LST across the urban gradients than in the urban agglomeration and across the province as a whole during the day. Indeed, Dheivasigamani (2020) noted that the correlation between NL and LST was greater in regions with highest and lowest actual NL values than in those with median values. Li et al. (2019) also found significant correlations for this variable within suburbs and beyond, as is the case for this study, especially in A, Su, and Sf.

The SHAP method lays the foundation for exploring and comparing spatial variation in the relative impact of factors influencing LST at various scales in Zhejiang province, including across gradients inside the urban agglomerations. The method assists in locating the most significant factors and their relative contributions in specific localities, an outcome that goes beyond the understanding of LST drivers based on other approaches. The results are potentially useful for management, particularly in targeting the variables that may be adjusted or manipulated in spatial planning. For example, parameters relating to greening (EVI) and pollution (AOD) are potentially subject to management intervention and, therefore, have a modulating impact on LST. EVI and MNDWI emerge as the most important drivers of nighttime LST in the city center, especially in AHB, and are therefore especially relevant for urban planning. Our method facilitates the estimation of thresholds according to their SHAP values that can in turn be used to highlight areas that should be prioritized by the authorities in terms of managing LST in the future (Figs. S1 and 15).

Knowledge of which factors to target — and in which localities — may be of considerable value to the provincial, regional, or local land use planning authorities, especially in the context of climate change.

#### Limitation and future work

In this study, the relative importance of key factors influencing LST was ranked and explicitly mapped using XGBoost and SHAP algorithm with three sampling levels. The pixel-based map of relative importance of different factors in Zhejiang province is developed within a framework of data-driven modeling. However, there are several limitations that need to be considered, and highlighting these may guide future work or applications of the methodology to other cases. Firstly, the dataset obtained is at a relatively low temporal-spatial resolution, especially regarding land surface temperature and meteorological factors that are influenced by clouds in this coastal province. Given the aim here, i.e., to highlight the advantages of the SHAP method in producing a higher resolution view of LST factors, mean LST for the year 2014 were adopted, and all selected factors were kept the same to establish the relations with both the daytime and night LST. More recent data at higher spatial and temporal resolution are required, especially under conditions of rapidly changing temperature and other environmental factors. Because of the excellent explanation of SHAP method for grid details, LST and its influencing factors with finer resolutions will promote more sophisticated

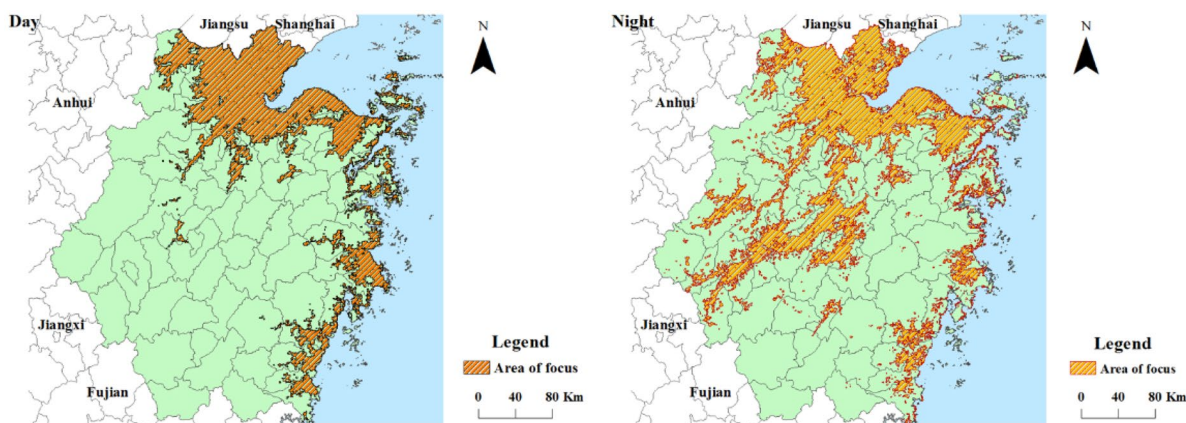


**Fig. 15** Daytime and nighttime area of interests

investigations. In the case of the urban environments, higher resolution images that capture building height/shadow and construction material would be more valuable (Huang & Wang, 2019; Liu et al., 2011; Yu et al., 2020). The complexity of building structure and its influence on LST should certainly be further investigated. Selection of summer and/or winter could also highlight seasonal impact as seen in other studies (Bala et al., 2020; Siddiqui et al., 2021). Spatio-temporal LST drivers are considered according to the baseline year of 2014. Secondly, further analysis of the interactions between different factors, not considered in this study (although see Fig. S2) may be conducted (Liu et al., 2021; Stirnberg et al., 2021). Thirdly, constrained by the limitations of the machine learning method, fundamental principles between LST and key factors may not have been fully accounted for, and some of the resultant spatial patterns are difficult to interpret (such as the orientation of SHAP values for longitude/latitude and the relative importance of NL (especially compared to NDBI even while these data are at higher spatial resolution)). Additional algorithms, incorporating conceptual models (Chakraborty & Lee, 2019) may improve the empirical performance of the model and increase the explanatory power of the method to understand the impact of key factors on LST.

## Conclusions

In this study, XGBoost and SHAP were used, taking 2014 as the baseline year, to evaluate how derived systematic drivers, including natural factors, social factors, and landscape indices influence LST in Zhejiang Province. A hierarchical sampling schedule based on pixel level SHAP calculation over the whole province was constructed to identify the most important factors and their spatially heterogeneous contributions. The main conclusions are as follows:

1. Urban centers hold the highest mean LST, followed by the urban agglomeration and the province. For the whole province, areas with higher LST values are generally located in the northeast, while lower temperatures are associated with the higher land in the southwest. All urban agglomerations exhibit higher mean LST values than that of the province as a whole, among which AHB

exhibits the lowest and WTC the highest temperatures in both daytime and at night. Within the gradients of each urban agglomeration, the average LST decreased outwards from A to Sp.

2. The contributions of key factors to daytime and nighttime LST are variable across different spatial scales. At the scale of the province, latitude, elevation and nightlight are the most prominent determinants of daytime LST, while latitude, longitude, and AOD are most significant at night. Within the urban agglomerations, the effect of vegetation related factors on the nighttime LST in AHB is significantly greater than at the provincial level, while longitude (i.e., distance from sea) is the most important factor in WTC, and AOD in CZ. In the urban centers, EVI and MNDWI are the most important influencing factors at night. In general, EVI, MNDWI, NL, and NDBI affect LST more prominently at small spatial scales when compared with AOD, latitude, and TOP. Moreover, the top factors at different scales are more stable in the daytime than at night.
3. The SHAP method is useful in describing the spatial heterogeneity in the relative importance of key factors underlying LST, which therefore indicates its value in guiding planning policy. Highly positive effects on daytime LST are evident in nightlight data from the urban centers, indicating that such areas should be prioritized by the authorities in terms of managing the urban heat island effect. SHAP values relating to atmospheric quality (AOD), especially in the industrial CZ region is strongly apparent and should be considered in future planning. The impacts of vegetation on daytime LST indicated by EVI and forest landscape indices are spatially variable, but the importance of tree cover in the promoting downtown LST regulation is clear.

**Acknowledgements** We sincerely thank the editor and anonymous reviewers for their valuable comments and suggestions to improve the quality of this paper.

**Author contribution** Hu Yuhong: conceptualization, methodology, validation, writing—original draft preparation, and software. Wu Chaofan: conceptualization, writing—original draft preparation, writing—review and editing, and funding acquisition. Michael E. Meadows: writing—review and editing. Feng Meili: writing—review and editing. All authors reviewed the manuscript.

**Funding** This research was funded by the Natural Science Foundation of Zhejiang Province (NO. LQ19D010007), Jinhua Science and Technology Research Program (NO. 2021-4-341) and Independent Design Scientific Research Project of Zhejiang Normal University (NO. 2021ZS0702).

**Data availability statement** All data are incorporated into the article and its online supplementary material.

## Declarations

**Ethics approval and consent to participate** No medical or animal experiments have been conducted, so ethics approval is not applicable. We affirm that all authors have participated in the research work and are fully aware of ethical responsibilities.

**Consent for publication** We affirm that all authors have agreed for the submission of the paper to EMAS and are fully aware of ethical responsibilities.

**Competing interest** The authors declare no competing interests.

## References

- Arnfield, A. J. (2003). Two decades of urban climate research: A review of turbulence, exchanges of energy and water, and the urban heat island. *International Journal of Climatology*, 23(1), 1–26. <https://doi.org/10.1002/joc.859>
- Bala, R., Prasad, R., & Pratap Yadav, V. (2020). A comparative analysis of day and night land surface temperature in two semi-arid cities using satellite images sampled in different seasons. *Advances in Space Research*, 66(2), 412–425. <https://doi.org/10.1016/j.asr.2020.04.009>
- Cai, Z., Han, G., & Chen, M. (2018). Do water bodies play an important role in the relationship between urban form and land surface temperature? *Sustainable Cities and Society*, 39, 487–498. <https://doi.org/10.1016/j.scs.2018.02.033>
- Carlson, T. N., Gillies, R. R., & Perry, E. M. (1994). A method to make use of thermal infrared temperature and NDVI measurements to infer surface soil water content and fractional vegetation cover. *Remote Sensing Reviews*, 9(1–2), 161–173. <https://doi.org/10.1080/02757259409532220>
- Chakraborty, T., & Lee, X. (2019). Land cover regulates the spatial variability of temperature response to the direct radiative effect of aerosols. *Geophysical Research Letters*, 46(15), 8995–9003. <https://doi.org/10.1029/2019GL083812>
- Chen, S., Yu, Z., Liu, M., Da, L., & Faiz ul Hassan, M. (2021). Trends of the contributions of biophysical (climate) and socio-economic elements to regional heat islands. *Scientific Reports*, 11(1), 12696. <https://doi.org/10.1038/s41598-021-92271-3>
- Chen, T., He, T., Benesty, M., Khotilovich, V., Tang, Y., Cho, H., & Chen, K. (2015). Xgboost: Extreme gradient boosting. *R package version 0.4–2*, 1(4), 1–4.
- Chen, Z., Gong, C., Wu, J., & Yu, S. (2012). The influence of socioeconomic and topographic factors on nocturnal urban heat islands: A case study in Shenzhen. *China. International Journal of Remote Sensing*, 33(12), 3834–3849. <https://doi.org/10.1080/01431161.2011.635717>
- Cheng, M., & Duan, C. (2021). The changing trends of internal migration and urbanization in China: new evidence from the seventh National Population Census. *China Population and Development Studies*, 5(3), 275–295. <https://doi.org/10.1007/s42379-021-00093-7>
- China Statistical Yearbook. (2015). Beijing: China Statistical Publishing House.
- Coutts, A. M., Beringer, J., & Tapper, N. J. (2007). Impact of increasing urban density on local climate: Spatial and temporal variations in the surface energy balance in Melbourne, Australia. *Journal of Applied Meteorology and Climatology*, 46(4), 477–493. <https://doi.org/10.1175/JAM2462.1>
- Cui, Y., Xu, X., Dong, J., & Qin, Y. (2016). Influence of urbanization factors on surface urban heat island intensity: A comparison of countries at different developmental phases. *Sustainability*, 8(8), 706. <https://doi.org/10.3390/su8080706>
- Deng, Y., Chen, R., Xie, Y., Xu, J., Yang, J., & Liao, W. (2021). Exploring the impacts and temporal variations of different building roof types on surface urban heat island. *Remote Sensing*, 13(14), 2840. MDPI AG. <https://doi.org/10.3390/rs13142840>
- Deng, Y., Wang, S., Bai, X., Tian, Y., Wu, L., Xiao, J., & Qian, Q. (2018). Relationship among land surface temperature and LUCC, NDVI in typical karst area. *Scientific Reports*, 8(1), 641. <https://doi.org/10.1038/s41598-017-19088-x>
- Dheivasigamani, P. (2020). *Relationship between nighttime lights and land surface temperature*. Retrieved May 21, 2022, from Deqing, Zhejiang, China: <https://a-a-r-s.org/proceeding/ACRS2020/ac2szp.pdf>
- Ezimand, K., Azadbakht, M., & Aghighi, H. (2021). Analyzing the effects of 2D and 3D urban structures on LST changes using remotely sensed data. *Sustainable Cities and Society*, 74, 103216. <https://doi.org/10.1016/j.scs.2021.103216>
- Fan, J., Wang, X., Wu, L., Zhou, H., Zhang, F., Yu, X., & Xiang, Y. (2018). Comparison of Support Vector Machine and Extreme Gradient Boosting for predicting daily global solar radiation using temperature and precipitation in humid subtropical climates: A case study in China. *Energy Conversion and Management*, 164, 102–111. <https://doi.org/10.1016/j.enconman.2018.02.087>
- Geng, S., Yang, L., Sun, Z., Wang, Z., Qian, J., Jiang, C., & Wen, M. (2021). Spatiotemporal patterns and driving forces of remotely sensed urban agglomeration heat islands in South China. *Science of The Total Environment*, 800, 149499. <https://doi.org/10.1016/j.scitotenv.2021.149499>
- Gillies, R. R., & Carlson, T. N. (1995). Thermal remote sensing of surface soil water content with partial vegetation cover for incorporation into climate models. *Journal of Applied Meteorology and Climatology*, 34(4), 745–756. [https://doi.org/10.1175/1520-0450\(1995\)034%3c0745:TRSOSS%3e2.0.CO;2](https://doi.org/10.1175/1520-0450(1995)034%3c0745:TRSOSS%3e2.0.CO;2)
- Gillies, R. R., Kustas, W. P., & Humes, K. S. (1997). A verification of the ‘triangle’ method for obtaining surface soil water content and energy fluxes from remote measurements of the Normalized Difference Vegetation Index (NDVI) and surface e. *International Journal of Remote Sensing*, 18(15), 3145–3166. <https://doi.org/10.1080/014311697217026>

- Gluch, R., Quattrochi, D. A., & Luvall, J. C. (2006). A multi-scale approach to urban thermal analysis. *Remote Sensing of Environment*, 104(2), 123–132. <https://doi.org/10.1016/j.rse.2006.01.025>
- Gu, Q., Wang, H., Zheng, Y., Zhu, J., & Li, X. (2015). Ecological footprint analysis for urban agglomeration sustainability in the middle stream of the Yangtze River. *Ecological Modelling*, 318, 86–99. <https://doi.org/10.1016/j.ecolmodel.2015.07.022>
- Hanhua, L., Zihan, Z., & Xiayun, P. (2016). Climatic characteristics of high temperatures in Zhejiang Province in 1951–2013. *Bulletin of Science and Technology*, 32(01), 59–64. <https://doi.org/10.13774/j.cnki.kjtb.2016.01.012>
- Hou, H., & Estoque, R. C. (2020). Detecting cooling effect of landscape from composition and configuration: An urban heat island study on Hangzhou. *Urban Forestry & Urban Greening*, 53, 126719. <https://doi.org/10.1016/j.ufug.2020.126719>
- Hu, L., & Brunsell, N. A. (2013). The impact of temporal aggregation of land surface temperature data for surface urban heat island (SUHI) monitoring. *Remote Sensing of Environment*, 134, 162–174. <https://doi.org/10.1016/j.rse.2013.02.022>
- Hu, Y., Hou, M., Jia, G., Zhao, C., Zhen, X., & Xu, Y. (2019). Comparison of surface and canopy urban heat islands within megacities of eastern China. *ISPRS Journal of Photogrammetry and Remote Sensing*, 156, 160–168. <https://doi.org/10.1016/j.isprsjprs.2019.08.012>
- Huang, X., & Wang, Y. (2019). Investigating the effects of 3D urban morphology on the surface urban heat island effect in urban functional zones by using high-resolution remote sensing data: A case study of Wuhan, Central China. *ISPRS Journal of Photogrammetry and Remote Sensing*, 152, 119–131. <https://doi.org/10.1016/j.isprsjprs.2019.04.010>
- Jin, M., Shepherd, J. M., & Zheng, W. (2010). Urban surface temperature reduction via the urban aerosol direct effect: A remote sensing and WRF model sensitivity study. *Advances in Meteorology*, 2010, 681587. <https://doi.org/10.1155/2010/681587>
- Karnieli, A., Agam, N., Pinker, R. T., Anderson, M., Imhoff, M. L., Gutman, G. G., & Goldberg, A. (2010). Use of NDVI and land surface temperature for drought assessment: Merits and limitations. *Journal of Climate*, 23(3), 618–633. <https://doi.org/10.1175/2009JCLI2900.1>
- Kim, J.-H., Gu, D., Sohn, W., Kil, S.-H., Kim, H., & Lee, D.-K. (2016). Neighborhood landscape spatial patterns and land surface temperature: An empirical study on single-family residential areas in Austin, Texas. *International Journal of Environmental Research and Public Health*, 13(9), 880. <https://doi.org/10.3390/ijerph13090880>
- Kim, M. J. (2019). Changes in the relationship between particulate matter and surface temperature in Seoul from 2002–2017. *Atmosphere*, 10(5). <https://doi.org/10.3390/atmos10050238>
- Kulcsár, L. J. (2013). Rural migration, Europe and North America 1945 to present. In I. Ness (Ed.), *The encyclopedia of global human migration*. <https://doi.org/10.1002/9781444351071.wbeghm463>
- Lai, J., Zhan, W., Quan, J., Liu, Z., Li, L., Huang, F., & Liao, W. (2021). Reconciling debates on the controls on surface urban heat island intensity: effects of scale and sampling. *Geophysical Research Letters*, 48(19), e2021GL094485. <https://doi.org/10.1029/2021GL094485>
- Li, J., Carlson, B. E., Yung, Y. L., Lv, D., Hansen, J., Penner, J. E., & Dong, Y. (2022). Scattering and absorbing aerosols in the climate system. *Nature Reviews Earth & Environment*, 3(6), 363–379. <https://doi.org/10.1038/s43017-022-00296-7>
- Li, J., Song, C., Cao, L., Zhu, F., Meng, X., & Wu, J. (2011). Impacts of landscape structure on surface urban heat islands: A case study of Shanghai. *China. Remote Sensing of Environment*, 115(12), 3249–3263. <https://doi.org/10.1016/j.rse.2011.07.008>
- Li, J., Wang, F., Fu, Y., Guo, B., Zhao, Y., & Yu, H. (2020a). A novel SUHI referenced estimation method for multicenters urban agglomeration using DMSP/OLS nighttime light data. *IEEE Journal of Selected Topics in Applied Earth Observations and Remote Sensing*, 13, 1416–1425. <https://doi.org/10.1109/JSTARS.2020.2981285>
- Li, L., Huang, X., Li, J., & Wen, D. (2017). Quantifying the spatiotemporal trends of canopy layer heat island (CLHI) and its driving factors over Wuhan, China with satellite remote sensing. *Remote Sensing*, 9(6). <https://doi.org/10.3390/rs9060536>
- Li, L., Yu, T., Zhao, L., Zhan, Y., Zheng, F., Zhang, Y., & Wang, C. (2019). Characteristics and trend analysis of the relationship between land surface temperature and nighttime light intensity levels over China. *Infrared Physics & Technology*, 97, 381–390. <https://doi.org/10.1016/j.infrared.2019.01.018>
- Li, L., Zha, Y., & Zhang, J. (2020b). Spatially non-stationary effect of underlying driving factors on surface urban heat islands in global major cities. *International Journal of Applied Earth Observation and Geoinformation*, 90, 102131. <https://doi.org/10.1016/j.jag.2020.102131>
- Li, X., Wu, C., Meadows, M. E., Zhang, Z., Lin, X., Zhang, Z., & Hu, Y. (2021). Factors underlying spatiotemporal variations in atmospheric PM2.5 concentrations in Zhejiang Province, China. *Remote Sensing*, 13(15), 3011. <https://doi.org/10.3390/rs13153011>
- Liu, W., Gong, A., Zhou, J., & Zhan, W. (2011). Investigation on relationships between urban building materials and land surface temperature through a multi-resource remote sensing approach. *Remote Sensing Information*, (04), 46–53.
- Liu, W., Meng, Q., Allam, M., Zhang, L., Hu, D., & Menenti, M. (2021). Driving factors of land surface temperature in urban agglomerations: A case study in the pearl river delta, china. *Remote Sensing*, 13(15), 2858. <https://doi.org/10.3390/rs13152858>
- Local Records Office of Zhejiang Provincial People's Government. Retrieved May 21, 2022, from <http://www.zjdfz.cn/tiptai.web/BookRead.aspx?bookid=201212082676>
- Logan, T. M., Zaitchik, B., Guikema, S., & Nisbet, A. (2020). Night and day: The influence and relative importance of urban characteristics on remotely sensed land surface temperature. *Remote Sensing of Environment*, 247, 111861. <https://doi.org/10.1016/j.rse.2020.111861>
- Lundberg, S. M., Erion, G. G., & Lee, S. -I. (2018). Consistent individualized feature attribution for tree ensembles. *Methods*, 5, 25. <https://doi.org/10.48550/arXiv.1802.03888>
- Lundberg, S. M., & Lee, S. -I. (2017). A unified approach to interpreting model predictions. *Proceedings of the Advances in Neural Information Processing Systems*, 4765–4774.
- Ma, Q., Wu, J., & He, C. (2016). A hierarchical analysis of the relationship between urban impervious surfaces and land surface temperatures: Spatial scale dependence, temporal variations,

- and bioclimatic modulation. *Landscape Ecology*, 31(5), 1139–1153. <https://doi.org/10.1007/s10980-016-0356-z>
- Maishella, A., Dewantoro, B. E., & Aji, M. (2020). Correlation analysis of urban development and land surface temperature using Google Earth Engine in Sleman Regency, Indonesia. *IOP Conference Series: Earth and Environmental Science*, 540, 012018. <https://doi.org/10.1088/1755-1315/540/1/012018>
- Mathew, A., Sarwesh, P., & Khandelwal, S. (2022). Investigating the contrast diurnal relationship of land surface temperatures with various surface parameters represent vegetation, soil, water, and urbanization over Ahmedabad city in India. *Energy Nexus*, 5, 100044. <https://doi.org/10.1016/j.nexus.2022.100044>
- Nations, U. (2018). Revision of world urbanization prospects. *United Nations: New York, NY, USA*, 799. Retrieved May 21, 2022, from <https://www.un.org/development/desa/publications/2018-revision-of-world-urbanization-prospects.html>
- Oke, T. R. (1982). The energetic basis of the urban heat island. *Quarterly Journal of the Royal Meteorological Society*, 108(455), 1–24. <https://doi.org/10.1002/qj.49710845502>
- Peng, J., Qiao, R., Liu, Y., Blaschke, T., Li, S., Wu, J., & Liu, Q. (2020). A wavelet coherence approach to prioritizing influencing factors of land surface temperature and associated research scales. *Remote Sensing of Environment*, 246, 111866. <https://doi.org/10.1016/j.rse.2020.111866>
- Peng, S., Piao, S., Ciais, P., Friedlingstein, P., Ottle, C., Bréon, F.-M., & Myneni, R. B. (2012). Surface urban heat island across 419 global big cities. *Environmental Science & Technology*, 46(2), 696–703. <https://doi.org/10.1021/es2030438>
- Pouyan, S., Rahamanian, S., Amindin, A., & Pourghasemi, H. R. (2022). Chapter 15 - spatial and seasonal modeling of the land surface temperature using random forest. In H. R. Pourghasemi (Ed.), *Computers in Earth and Environmental Sciences* (pp. 221–234). Elsevier.
- Rongping, L., Xinhua, Q., & Shilin, Y. (2017). Spatial-temporal characteristics of urban heat islands and driving mechanisms in a coastal valley-basin city: A case study of Fuzhou City. *Acta Ecologica Sinica*, 37(01), 294–304.
- Sharma, I., Tongkumchum, P., & Ueranantasun, A. (2018). Modeling of land surface temperatures to determine temperature patterns and detect their association with altitude in the Kathmandu Valley of Nepal. *Chiang Mai University Journal of Natural Sciences*, 17(4), 275–288. <https://doi.org/10.12982/CMUJNS.2018.0020>
- Shenglong, W. E. I., Zhibiao, C., Zhiqiang, C., Qiuyun, W., Xiuli, M. A., & Xinyu, Y. A. N. (2017). Simulation of the total solar radiation over micro-landform and correlation between the solar radiation and the land surface temperature. *Remote Sensing for Land & Resources*, 1(1), 129–135. <https://doi.org/10.6046/gtzyyg.2017.01.20>
- Siddiqui, A., Kushwaha, G., Nikam, B., Srivastav, S. K., Shelar, A., & Kumar, P. (2021). Analysing the day/night seasonal and annual changes and trends in land surface temperature and surface urban heat island intensity (SUHII) for Indian cities. *Sustainable Cities and Society*, 75, 103374. <https://doi.org/10.1016/j.scs.2021.103374>
- Sobrino, J. A., & Irakulis, I. (2020). A methodology for comparing the surface urban heat island in selected urban agglomerations around the world from sentinel-3 SLSTR data. *IJ*(12), 2052. <https://doi.org/10.3390/rs12122052>
- Soydan, O. (2020). Effects of landscape composition and patterns on land surface temperature: Urban heat island case study for Nigde, Turkey. *Urban Climate*, 34, 100688. <https://doi.org/10.1016/j.uclim.2020.100688>
- Stirnberg, R., Cermak, J., Kotthaus, S., Haefelin, M., Andersen, H., Fuchs, J., & Favez, O. (2021). Meteorology-driven variability of air pollution (PM1) revealed with explainable machine learning. *Atmospheric Chemistry and Physics*, 21(5), 3919–3948.
- Taripanah, F., & Ranjbar, A. (2021). Quantitative analysis of spatial distribution of land surface temperature (LST) in relation ecohydrological, terrain and socio-economic factors based on Landsat data in mountainous area. *Advances in Space Research*, 68(9), 3622–3640. <https://doi.org/10.1016/j.asr.2021.07.008>
- Tayyebi, A., Shafizadeh-Moghadam, H., & Tayyebi, A. H. (2018). Analyzing long-term spatio-temporal patterns of land surface temperature in response to rapid urbanization in the mega-city of Tehran. *Land Use Policy*, 71, 459–469. <https://doi.org/10.1016/j.landusepol.2017.11.023>
- Venter, Z. S., Chakraborty, T., & Lee, X. (2021). Crowd-sourced air temperatures contrast satellite measures of the urban heat island and its mechanisms. *Science Advances*, 7(22), eabb9569. <https://doi.org/10.1126/sciadv.eabb9569>
- Wang, Q., Wang, X., Zhou, Y., Liu, D., & Wang, H. (2022). The dominant factors and influence of urban characteristics on land surface temperature using random forest algorithm. *Sustainable Cities and Society*, 79, 103722. <https://doi.org/10.1016/j.scs.2022.103722>
- Wang, Y., Yi, G., Zhou, X., Zhang, T., Bie, X., Li, J., & Ji, B. (2021a). Spatial distribution and influencing factors on urban land surface temperature of twelve megacities in China from 2000 to 2017. *Ecological Indicators*, 125, 107533. <https://doi.org/10.1016/j.ecolind.2021.107533>
- Wang, Z., Meng, Q., Allam, M., Hu, D., Zhang, L., & Menenti, M. (2021b). Environmental and anthropogenic drivers of surface urban heat island intensity: A case-study in the Yangtze River Delta, China. *Ecological Indicators*, 128, 107845. <https://doi.org/10.1016/j.ecolind.2021.107845>
- Wolf, K. L., Ahn, C., & Noe, G. B. (2011). Microtopography enhances nitrogen cycling and removal in created mitigation wetlands. *Ecological Engineering*, 37(9), 1398–1406. <https://doi.org/10.1016/j.ecoleng.2011.03.013>
- Xiali, L., Sheng, W., Shanrui, H., Xiaoting, L., Wenyu, Y., Maosong, L., & Chi, X. (2018). A multi-scale study on the formation mechanism and main controlling factors of urban thermal field based on urban big data. *Chinese Journal of Applied Ecology*, 29(09), 2861–2868.
- Xiang, Y., Huang, C., Huang, X., Zhou, Z., & Wang, X. (2021). Seasonal variations of the dominant factors for spatial heterogeneity and time inconsistency of land surface temperature in an urban agglomeration of central China. *Sustainable Cities and Society*, 75, 103285. <https://doi.org/10.1016/j.scs.2021.103285>
- Xiang, Y., Ye, Y., Peng, C., Teng, M., & Zhou, Z. (2022). Seasonal variations for combined effects of landscape metrics on land surface temperature (LST) and aerosol optical depth (AOD). *Ecological Indicators*, 138, 108810. <https://doi.org/10.1016/j.ecolind.2022.108810>

- Xin, W., Bin, L., Min, L., & Ruina, S. (2021). Combination of LightGBM and SHAP for diabetes prediction and feature analysis. *Journal of Chinese Computer Systems*, 1–11. Retrieved Retrieved May 21, 2022, from <https://kns.cnki.net/kcms/detail/21.1106.tp.20210906.1452.031.html>
- Yang, L., Yu, K., Ai, J., Liu, Y., Yang, W., & Liu, J. (2022). Dominant factors and spatial heterogeneity of land surface temperatures in urban areas: A case study in Fuzhou, China. *Remote Sensing*, 14(5), 1266. MDPI AG. <https://doi.org/10.3390/rs14051266>
- Yang, Z., Fuhamo, Z., & Cai, c., Guanqi, J., Agen, Q., & Geli, O. (2021). Analysis of characteristics and influencing factors of atmospheric visibility in Beijing-Tianjin-Hebei region. *Science of Surveying and Mapping*, 46(07), 196–204. <https://doi.org/10.16251/j.cnki.1009-2307.2021.07.027>
- Yiman, L., Chunliang, X., Ye, W., & Pingjun, S. (2016). Spatial evolution of organization and structure of three major urban agglomerations in Zhejiang Province. *Economic Geography*, 36(11), 47–53. <https://doi.org/10.15957/j.cnki.jjdl.2016.11.007>
- Yu, S., Chen, Z., Yu, B., Wang, L., Wu, B., Wu, J., & Zhao, F. (2020). Exploring the relationship between 2D/3D landscape pattern and land surface temperature based on explainable eXtreme Gradient Boosting tree: A case study of Shanghai, China. *Science of The Total Environment*, 725, 138229. <https://doi.org/10.1016/j.scitotenv.2020.138229>
- Yu, Y., Shang, G., Duan, S., Yu, W., Labed, J., & Li, Z. (2022). Quantifying the influences of driving factors on land surface temperature during 2003–2018 in China using convergent cross mapping method. *Remote Sensing*, 14(14), 3280. MDPI AG. <https://doi.org/10.3390/rs14143280>
- Yu, Z., Yao, Y., Yang, G., Wang, X., & Vejre, H. (2019). Strong contribution of rapid urbanization and urban agglomeration development to regional thermal environment dynamics and evolution. *Forest Ecology and Management*, 446, 214–225. <https://doi.org/10.1016/j.foreco.2019.05.046>
- Yundong, G., & Hao, L. (2021). Load forecasting based on optimal feature combination improved XGBoost. *Application Research of Computers*, 38(09), 2767–2772. <https://doi.org/10.19734/j.issn.1001-3695.2020.12.0552>
- Yunfang, J., Cong, Y., Tiemao, S., & Danran, S. (2018). *Spatial analysis of the cooling effect of urban small rivers on residential districts*. Paper presented at the 2018 China Urban Planning Annual Conference Hangzhou, Zhejiang, China.
- Zheng, Z., Zeng, Y., Li, S., & Huang, W. (2016). A new burn severity index based on land surface temperature and enhanced vegetation index. *International Journal of Applied Earth Observation and Geoinformation*, 45, 84–94. <https://doi.org/10.1016/j.jag.2015.11.002>
- Zhi, Y., Shan, L., Ke, L., & Yang, R. (2020). Analysis of land surface temperature driving factors and spatial heterogeneity research based on geographically weighted regression model. *Complexity*, 2020, 2862917. <https://doi.org/10.1155/2020/2862917>
- Zhiyu, F., Qingming, Z., Huimin, L., Chen, Y., & Yu, X. (2019). Spatial-temporal distribution of urban heat island and the heating effect of impervious surface in summer in Wuhan. *Journal of Geo-Information Science*, 21(02), 226–235.
- Zhou, D., Zhao, S., Liu, S., Zhang, L., & Zhu, C. (2014). Surface urban heat island in China's 32 major cities: Spatial patterns and drivers. *Remote Sensing of Environment*, 152, 51–61. <https://doi.org/10.1016/j.rse.2014.05.017>
- Zhou, L., Hu, F., Wang, B., Wei, C., Sun, D., & Wang, S. (2022). Relationship between urban landscape structure and land surface temperature: Spatial hierarchy and interaction effects. *Sustainable Cities and Society*, 80, 103795. <https://doi.org/10.1016/j.scs.2022.103795>

**Publisher's Note** Springer Nature remains neutral with regard to jurisdictional claims in published maps and institutional affiliations.

Springer Nature or its licensor (e.g. a society or other partner) holds exclusive rights to this article under a publishing agreement with the author(s) or other rightsholder(s); author self-archiving of the accepted manuscript version of this article is solely governed by the terms of such publishing agreement and applicable law.